

Mixed Parallel–Perpendicular Morphologies in Diblock Copolymer Systems Correlated to the Linear Viscoelastic Properties of the Parallel and Perpendicular Morphologies

B. Scott Pinheiro and Karen I. Winey*

Department of Materials Science and Engineering, Laboratory for Research on the Structure of Matter, University of Pennsylvania, Philadelphia, Pennsylvania 19104-6272

Received February 6, 1998; Revised Manuscript Received May 4, 1998

ABSTRACT: Large-amplitude oscillatory shear (LAOS) has been applied to a lamellar, microphase-separated, low molecular weight poly(styrene-*b*-isoprene) diblock copolymer melt to induce macroscopically aligned morphologies. Small-angle X-ray scattering and dynamic mechanical testing were performed to characterize the states of orientation. The perpendicular orientation was induced by applying LAOS at a fixed frequency (1 rad/s) and strain amplitude (100%) at high temperatures. LAOS applied at the same frequency and strain amplitude but at lower temperatures induced the parallel orientation. Interestingly, intermediate temperatures produced a mixed morphology containing both parallel and perpendicular orientations. The linear viscoelastic responses of the parallel and perpendicular morphologies were related to the LAOS conditions necessary to produce the perpendicular, the parallel, and the mixed parallel–perpendicular morphologies. Specifically, two frequencies were defined using the linear viscoelastic responses: $\omega_{Pd-P'}$ where $G'(\text{parallel}) = G'(\text{perpendicular})$ and $\omega_{Pd-P''}$ where $G''(\text{parallel}) = G''(\text{perpendicular})$. The uniaxial morphology induced by LAOS was found to correspond to that morphology which subsequently produced the lowest linear viscoelastic moduli, both elastic and storage. Analysis also showed that the viscoelastic response of the mixed parallel–perpendicular morphology could be approximated by a linear combination of the responses for samples wholly in the parallel and perpendicular orientations. Similar alignment and rheological results were obtained for a blend containing the diblock copolymer and 10 wt % homopolystyrene.

I. Introduction

Microphase-separated block copolymers are in essence self-assembled composites on a nanometer size scale. Some of the scientific and technical interest in studying these systems derives from the potential to design into them novel permeability, optical, electrical, or mechanical properties. Applying strong shear fields to microphase-separated block copolymer melts has been shown to macroscopically align the microdomains into a common orientation throughout a sample.^{1–15} For the case of the lamellar morphology, subjecting specimens to large-amplitude oscillatory shear (LAOS) under different experimental conditions can induce two types of macroscopic, uniaxial orientation:^{5–8,10,13,14,16–19} parallel, in which the planes of the lamellae are oriented parallel to the shearing surfaces, and perpendicular, in which the planes are oriented perpendicular to the shearing surfaces but contain the shearing direction (Figure 1). The potential for commercial applications is increased by this ability to induce macroscopic alignment of the microdomains throughout the bulk. In order to obtain better control over the perfection of orientation, an improved understanding of the alignment mechanisms is needed.

The progression from an unaligned to a uniaxially aligned block copolymer is inherently complex. Much of the difficulty in unraveling this problem stems from the number of pertinent experimental variables (shear frequency, strain amplitude, duration of shear, temperature, materials characteristics), most of which have been at least partially addressed. Each of these variables does not necessarily have a unique and independent affect on the mechanism of alignment. For example, increasing the strain amplitude in a dynamic

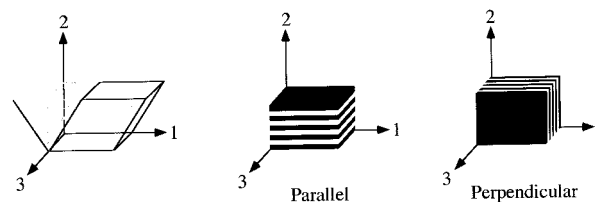


Figure 1. Shearing coordinates in which 1 is the shear direction, 2 is the shear gradient direction, and 3 is the neutral direction. Parallel and perpendicular orientations of lamellar diblock copolymers relative to the shearing coordinates.

experiment while keeping the frequency constant also has the effect of increasing the velocity of shear (shear rate), which, in turn, affects the apparent viscosity. The apparent viscosity can also be altered in a dynamic experiment by changing the frequency or in the case of this study by changing the temperature. In the ensuing discussion our results will be shown to lend support to theoretical work which indicates that the relative viscosities (i.e., viscoelastic contrast) of the microdomains are important in controlling the induced orientation.

In this study we further explore the phenomenon of macroscopic alignment through varying the temperature at which LAOS is applied. Typically, only the proximity of the LAOS condition to the microphase separation transition temperature has been considered. Undeniably, the “strength of segregation” when LAOS is applied will have an influence on the alignment induced; however, in a system, such as ours, where viscoelastic contrast exists, we suggest that the LAOS temperature’s influence on the viscosity of the microdomains must also be taken into account.

In this paper, two experimental systems are studied: a neat poly(styrene-*b*-isoprene) diblock copolymer and a binary blend of this diblock with 10 wt % homopoly-styrene. The data from both systems qualitatively exhibit the same trends. In an effort to reduce redundancy, the text of this paper will refer primarily to the neat system.

II. Experimental Section

Materials. Both of the polymers used in this study were purchased from Pressure Chemical Co. (Pittsburgh, PA). The lamellar poly(styrene-*b*-isoprene) diblock copolymer, SI(11–10), has PS and PI block molecular weights of 11 100 and 10 100 g/mol, respectively, a molecular weight polydispersity of $M_w/M_n = 1.03$, and a polystyrene volume fraction of $f_s = 0.505$. A blend of this diblock copolymer was prepared with 10 wt % of a homopolystyrene (13 500 g/mol, $M_w/M_n = 1.06$) and is designated as SI(11–10)/hS(13) 10%. Blend preparation involved creating a dilute solution (~3 wt %) in toluene, evaporating at room conditions (7–10 days), and two-stage drying under vacuum (40 °C for 1 day, 120 °C for ~3 days). Using a Perkin-Elmer system 7 DSC, the glass transition temperatures of the PS microdomains were determined for the neat diblock and the blend to be 76 and 79 °C, respectively. Using the optical birefringence technique described by Balsara et al.,²⁰ the ODT temperatures were determined for the neat diblock and the blend to be 157 and 162 °C, respectively. (T_g and T_{ODT} values for additional blends are reported elsewhere^{21,22} and are consistent with previous findings.²³)

SAXS. Small-angle X-ray scattering (SAXS) was performed using a reconditioned and upgraded Elliot GX-6 rotating anode (Cu K α) operated at 40 kV with a 0.2×2 mm microfocus cathode, pinhole optics, and Ni foil monochromation. A Siemens HiStar 2 D detector was used at the end of a 60-cm, He-filled flight path. Angular calibration of the detector was accomplished initially with a wet collagen specimen from a fresh rat tail which has a repeat distance of 66.8 nm. Angular calibration was performed on a daily basis with a dried and stained collagen specimen from a duck's tendon which has a repeat distance of 60.9 nm and exhibits 10 orders of reflections. Scattering experiments were performed in the three principal directions relative to the shearing direction (Figure 1): 1, velocity direction; 2, velocity gradient; and 3, neutral direction. Because these three, real-space directions are mutually orthogonal, the reciprocal-space directions, which are denoted by an asterisk, are parallel to the real-space directions. Samples were cut as necessary so that the path length through the sample was ~1 mm.

Rheology. A Rheometrics solids analyzer, RSAII (sinusoidal shear, shear sandwich geometry, 0.5 mm sample thickness), was used both to measure the dynamic mechanical properties of the copolymer and to induce macroscopic orientation in the samples. The sample chamber of the rheometer was under a constant N₂ purge to guard against oxidative degradation at elevated temperatures. SEC tests performed before and after the rheological tests indicate that no detectable sample degradation occurred.

Prior to rheological testing, the specimens were annealed in the rheometer ~2 °C above the ODT for several minutes (~5 min) and then cooled to 110 °C and held for ~15 min to allow the microphase-separated morphology to develop. This protocol reproducibly creates an initial isotropic state as confirmed by SAXS and rheological characterization.²² The rheological response was measured in the linear viscoelastic region by isothermal frequency sweeps with a strain amplitude of $\gamma = 1\%$. This is sufficiently small so as not to affect the rheological response by altering the state of macroscopic alignment. Then in an attempt to induce macroscopic alignment, specimens in the isotropic state were subjected to large-amplitude oscillatory shearing (LAOS) with a frequency of $\omega = 1$ rad/s and $\gamma = 98\%$. LAOS was applied for 1 h at one of the following constant temperatures: 100, 110, 115, 120, and 130 °C. These temperatures are above the glass transition

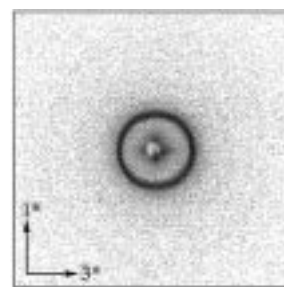


Figure 2. Representative two-dimensional SAXS pattern of the initial (isotropic) morphology of SI(11–10). The intensity scale for this and all subsequent 2D SAXS patterns is logarithmic. The first-order scattering maximum is visible (d spacing = 17.7 ± 0.2 nm).

temperature of the PS microdomains and below the microphase separation transition. Shearing at these LAOS conditions for longer times does not noticeably alter the morphologies as measured by SAXS and rheological characterization.²² After LAOS, specimens were annealed in the rheometer for 3 h at 110 °C before the final state was characterized. This annealing protocol is sufficient to allow the rheological response to reach a steady state.²² Master curves were obtained by shifting the data along the frequency axis after a vertical correction of T_0/T was applied to the modulus. The shift factors used to generate these master curves were well fit by the WLF equation.

III. Results

SAXS. The initial state of the SI(11–10) diblock copolymer is characterized in part by the representative 2D scattering pattern of Figure 2. The relative peak positions of the Bragg reflections as a function of scattering angle correspond to a lamellar microstructure. The uniform ring of scattered intensity at a fixed scattering angle indicates that the lamellar microdomains are randomly oriented throughout the bulk. SAXS patterns taken in three orthogonal directions confirm the identification of this initial state as isotropic. The lamellae in SI(11–10) and SI(11–10)/hS(13) 10% have long periods (d spacing) of 17.7 ± 0.2 and 18.0 ± 0.2 nm, respectively. These same d spacings are observed in all of the lamellar orientations induced by shearing in this study. This is not to imply the absence of lamellar contraction during LAOS as reported previously.^{12,24} However, the morphologies reported in this work are for specimens which have been fully “relaxed” by annealing for 3 h at 110 °C after cessation of LAOS.

The macroscopic state of orientation induced in SI(11–10) after it has been subjected to large-amplitude oscillatory shearing (LAOS) at 100 °C, as described above, is characterized by the three orthogonal scattering patterns in Figure 3. The scattering maximum along the 2* direction, and only along 2*, indicates that the parallel orientation has been induced by this shearing history. Figure 4a depicts the intensity distribution of the first-order maximum in the 2*–3* scattering plane (Figure 3c) as a function of the azimuthal angle. Scattering due to the parallel orientation (PI) is centered about an angle of 180°. After LAOS at 120 °C scattering patterns display intensity maxima along the 3* direction, and only along 3*, indicating that the perpendicular orientation (Pd) has been induced. This is evidenced by the scattered intensity centered about an azimuthal angle of 90° in the 2*–3* plane (Figure 4a).

The scattering patterns for specimens after LAOS at two intermediate temperatures, 110 and 115 °C, display significantly biaxial textures, containing both the paral-

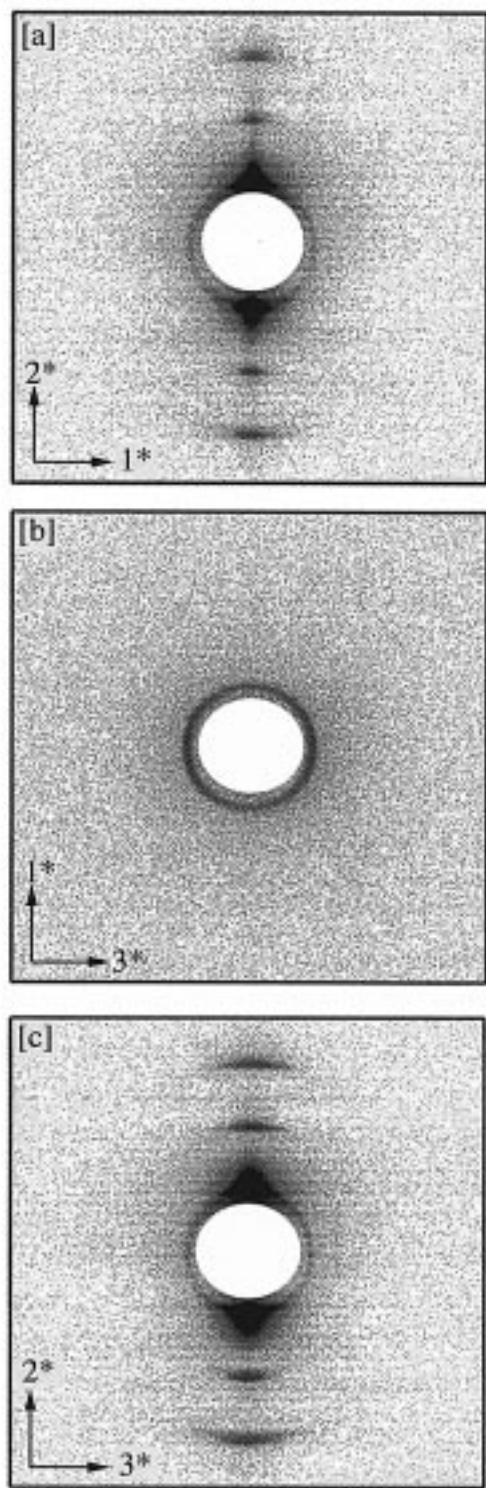


Figure 3. Orthogonal SAXS patterns for SI(11-10) after large-amplitude oscillatory shear (LAOS) at 100 °C indicating a parallel orientation. Patterns correspond to the incident X-ray beam along the neutral (a), gradient (b), and velocity (c) rheological directions.

lel and perpendicular orientations, (Figure 4a). The increased scattering centered about these two orientations is superposed on a weak ring of scattering, indicating the presence of lamellae with normals in the 2^*-3^* plane at orientations between the parallel and perpendicular orientations. For this reason these morphologies are referred to as "mixed" parallel-perpendicular instead of simply biaxial. SAXS patterns were

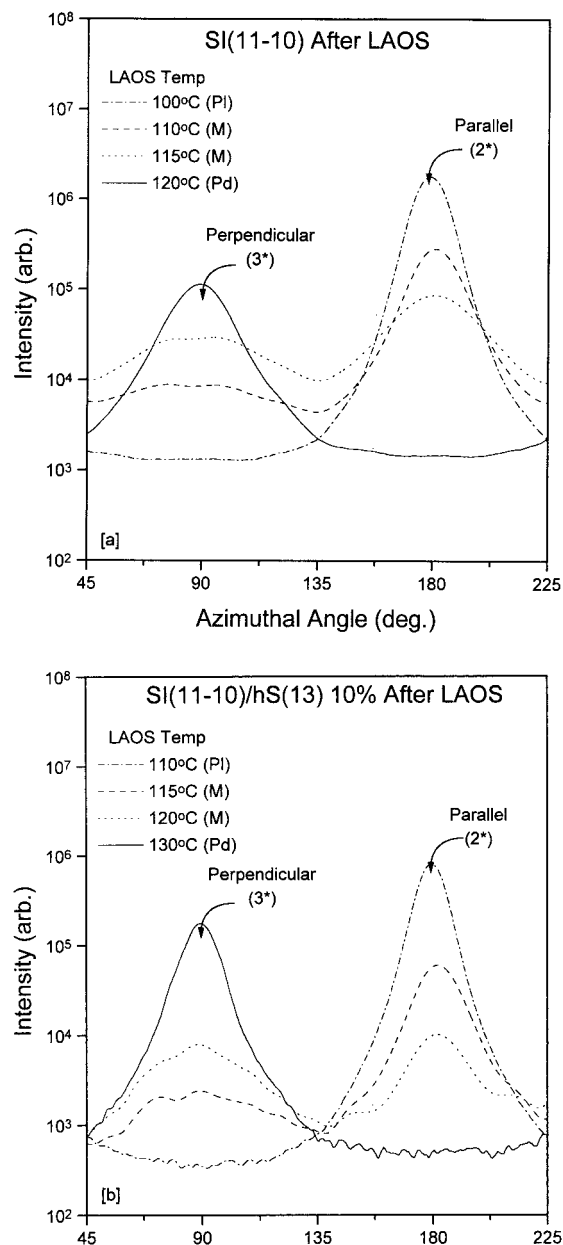


Figure 4. Azimuthal distribution of scattered intensity observed in the 2^*-3^* plane of SAXS patterns for (a) SI(11-10) and (b) SI(11-10)/hS(13) 10%. The data were integrated radially about the first-order diffraction maximum. Each curve represents data from a specimen after it was subjected to LAOS at the temperature shown in the legend and subsequently annealed. The azimuthal angles of 90° and 180° correspond to the 3^* (neutral) and 2^* (gradient) directions, respectively. These LAOS conditions produce the following morphologies: Pl, parallel orientation; Pd perpendicular orientation; M, mixed morphologies containing a combination of both parallel and perpendicular orientations.

taken of the mixed morphologies (M) in all three orthogonal directions and show no appreciable scattering due to lamellae in the transverse orientation.

LAOS applied at 110 °C produces a mixed morphology in which the scattering associated with the parallel orientation ($z = 180^\circ$) is significantly greater than that due to the perpendicular orientation. One measure of this is the ratio of the peak intensities at 180° to that at 90° which is $I_{Pl}:I_{Pd} \sim 34:1$. After LAOS at 115 °C, scattering due to the parallel orientation is only slightly greater than that due to the perpendicular orientation;

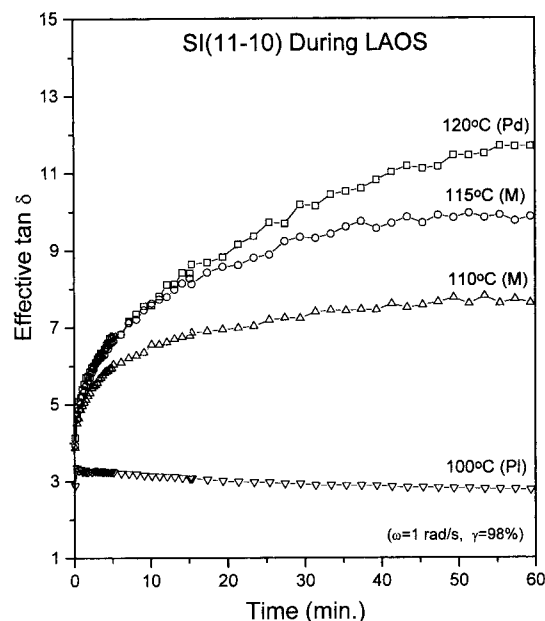


Figure 5. Effective loss tangent, $\tan \delta$, of SI(11–10) during LAOS ($\omega = 1$ rad/s, $\gamma = 98\%$) at each of the following temperatures: 100, 110, 115, and 120 °C.

$I_{PI}:I_{PD} \sim 3:1$. For comparison, the macroscopically parallel and perpendicular orientations, after LAOS at 100 and 120 °C, respectively, have intensity ratios of $I_{PI}:I_{PD} \sim 1300:1$ and $I_{PI}:I_{PD} \sim 1:80$, respectively.

Figure 4b displays the azimuthal intensity distributions of the first-order maximum in the $2^* - 3^*$ plane for SI(11–10) blended with 10 wt % hS(13). LAOS at 110 °C induces the parallel orientation of $I_{PI}:I_{PD} \sim 2300:1$; LAOS at 130 °C induces the perpendicular orientation of $I_{PI}:I_{PD} \sim 1:380$; LAOS at 115 and 120 °C induces mixed morphologies of $I_{PI}:I_{PD} \sim 25:1$ and $I_{PI}:I_{PD} \sim 1.3:1$, respectively. These results for the blend are similar to those found in the neat system. Again, these identifications of the macroscopic orientations were confirmed by SAXS patterns taken in all three orthogonal directions.

Rheology. Many previous studies have shown that subjecting lamellar microphase-separated block copolymers to LAOS alters the rheological response of the specimens.^{5–7,9–15} In general, the changes in dynamic mechanical response are typified by a decay in the moduli (G' , G'') (or more precisely the effective moduli) during shearing and only a partial recovery during subsequent annealing. Given that the moduli of a polymer are functions of temperature, it is inconvenient to use moduli as the comparative parameters to monitor changes when LAOS is applied at different temperatures. In contrast, $\tan \delta$ simplifies the comparison between experiments which were performed at different temperatures, because $\tan \delta (=G''/G')$ is a dimensionless parameter which measures the relative amount of stored and dissipated energy. Thus, during LAOS we monitor the changing rheological response of a specimen by using $\tan \delta$. As is the case of measuring the moduli during LAOS, $\tan \delta$ values recorded during LAOS are effective $\tan \delta$ values because the strain amplitude is greater than the linear viscoelastic limit.

Figure 5 displays the effective $\tan \delta$ for SI(11–10) subjected to LAOS at 100, 110, 115, and 120 °C. During LAOS at 100 °C (which induces the parallel orientation), $\tan \delta$ initially increases, then decreases, and eventually reaches a time-independent value. In contrast, during

LAOS at 120 °C (which induces the perpendicular orientation), $\tan \delta$ initially increases rapidly and then approaches a limiting value. During LAOS at intermediate temperatures of 110 and 115 °C (which induce mixed morphologies), $\tan \delta$ lies between those observed during the inducement of the parallel and perpendicular orientations. The data at 115 °C more closely resemble the $\tan \delta$ values corresponding to the production of the perpendicular orientation (120 °C) than do the 110 °C data. At these intermediate LAOS temperatures the effective $\tan \delta$ curves reach time-independent values, which is interpreted as indicating that a rheological “steady state” has been achieved. A few samples were subjected to LAOS for >1 h and verify that the rheological response had, in fact, become time-independent during the first hour of LAOS.²² Similar results were found for the blends. Note that while studying a similar material, Chen et al. found that longer times are necessary to develop a time independent birefringence.^{13,14}

Figure 6a compares the frequency dependence of the dynamic storage modulus G' for SI(11–10) in the isotropic state with that for the specimens after being subjected to LAOS ($\omega = 1$ rad/s, $\gamma = 98\%$, 1 h) at various temperatures followed by a 3 h anneal at 110 °C. Comparisons between the macroscopically isotropic, parallel, and perpendicular states will be discussed in a separate paper.^{21,22} At present it suffices to note that these three macroscopic morphologies each exhibit a unique viscoelastic response independent of the path used to create that morphology. For example, SI(11–10) specimens in the perpendicular orientation have a viscoelastic response identical with that shown in Figure 6a (Δ) regardless of whether LAOS was performed at 120 or 130 °C to create the perpendicular orientation. The specimens subjected to LAOS at 110 and 115 °C display moduli which lie between the responses for the parallel (100 °C) and perpendicular (120 °C) orientations. Figure 6b presents the corresponding data for the blend SI(11–10)/hS(13) 10%. Similar to the neat system, the specimens subjected to LAOS at intermediate temperatures of 115 and 120 °C display moduli which lie between the responses for the parallel (110 °C) and perpendicular (130 °C) orientations.

“Flipping” of the perpendicular orientation to the parallel orientation has been reported previously in low molecular weight SI diblock copolymers.^{10,16} A specimen of SI(11–10) was first aligned into the perpendicular orientation by LAOS at 130 °C. It was then subjected to LAOS at 100 °C, and the orientation was converted to the parallel orientation. The viscoelastic response of this specimen in the parallel orientation is identical to that shown in Figure 6a (\square), again demonstrating the path independence. However, reverse flipping, from parallel to perpendicular, was not observed, consistent with previous reports.^{10,16} For example, after aligning an SI(11–10) specimen into the parallel orientation, the parallel orientation persisted during LAOS at 130 °C.

IV. Discussion

Rheology of the Mixed Morphologies. The linear viscoelastic response of the mixed state is intermediary between the responses for the parallel and perpendicular orientations. This is as expected (assuming that the strain is distributed uniformly) given that the mixed state contains lamellae in both of these orientations. In fact, the viscoelastic response of the mixed morphology

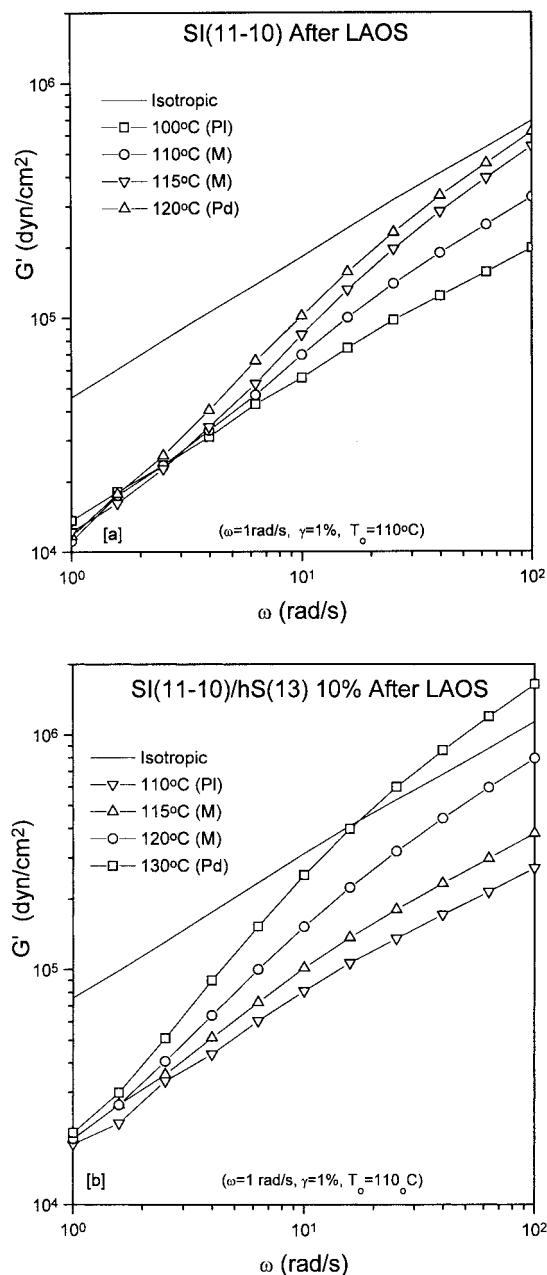


Figure 6. Linear viscoelastic dynamic storage modulus as a function of frequency for (a) SI(11-10) and (b) SI(11-10)/hS(13) 10%. Curves correspond to specimens after LAOS at the various temperatures shown in the legend and subsequent annealing. For comparison the moduli of the neat diblock copolymer and the blend are plotted for specimens having the isotropic morphology.

can be quantitatively described as a combination of the responses from these two principle orientations. Specifically, the moduli of the mixed state, G'_{MIX} and G''_{MIX} , can be approximated by a linear combination of the experimental data from a specimen in the parallel orientation, G'_{PI} , with that from a specimen in the perpendicular orientation, G'_{PD} , by the equations

$$G'_{\text{MIX}} = f_R G'_{\text{PI}} + (1 - f_R) G'_{\text{PD}} \quad (1)$$

$$G''_{\text{MIX}} = f_R G''_{\text{PI}} + (1 - f_R) G''_{\text{PD}} \quad (2)$$

where f_R is the fractional contribution due to the parallel orientation. A representative example of this analysis

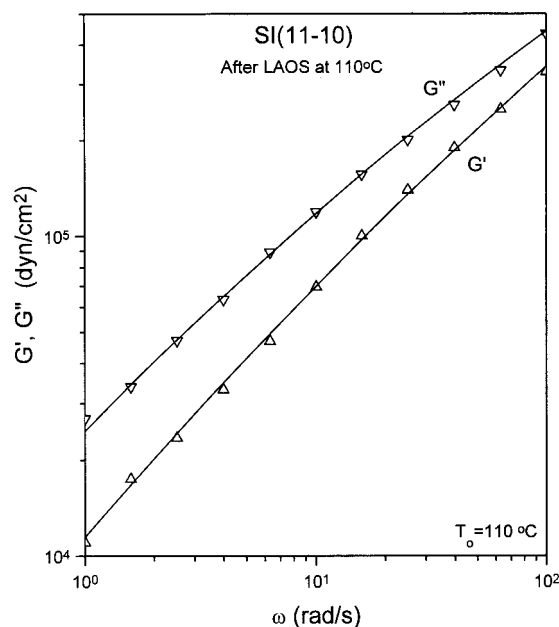


Figure 7. Dynamic storage (G') and loss (G'') moduli versus frequency. Symbols represent data for SI(11-10) after LAOS at 110 °C and subsequent annealing. Solid lines are a linear combination of the moduli for the parallel and perpendicular orientations calculated by eqs 1 and 2 using $f_R = 0.65$.

Table 1. Fractional Contributions Due to the Parallel Orientation within Mixed Morphology Specimens

sample	T_{LAOS} (°C)	f_R^a	f_{SAXS}^b
SI(11-10)	110	0.65	0.95
SI(11-10)	115	0.25	0.65
SI(11-10)/hS(13) 10%	115	0.90	0.90
SI(11-10)/hS(13) 10%	120	0.60	0.60

^a From rheological data using a linear fit of moduli; see eqs 1 and 2. ^b From SAXS data using areas under peaks in the azimuthal direction; see the text.

is displayed in Figure 7 where the symbols mark the experimental data for the SI(11-10) specimen after it has been subjected to LAOS at 110 °C and the solid lines were generated by eqs 1 and 2 with $f_R = 0.65$. For each specimen, a single value of f_R produces good agreement with both G' and G'' data. Table 1 reports the rheologically determined weighting coefficients, f_R , for the mixed morphology specimens studied in the neat system and the blend. The good agreement between the experimental data and the empirical fit supports the validity of using a linear combination of the parallel and perpendicular moduli to describe the mixed morphology moduli. This empirical construction suggests that the lamellar domains in the different orientations are responding additively and independently of each other.

The fractional contribution of the parallel orientation to the rheological response, f_R , is now compared with the fractional presence of the parallel orientation within a mixed morphology. The quantity of lamellae in or near a particular macroscopic orientation is estimated by the area, A , under a scattering peak in the azimuthal direction of a 2D SAXS pattern. The areas were calculated by an azimuthal integration of the first-order peaks in the 2^*-3^* plane, as shown in Figure 4. The approximate amounts of the parallel orientation relative to the perpendicular orientation, given by $f_{\text{SAXS}} = A_{\text{PI}} / (A_{\text{PI}} + A_{\text{PD}})$, are listed in Table 1 for the mixed morphologies.

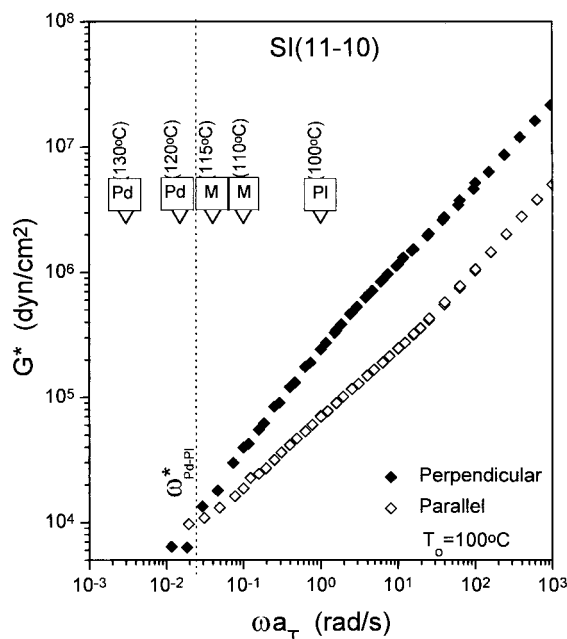


Figure 8. Master curves of the dynamic complex modulus (G^*) versus frequency for SI(11-10) samples in the parallel and perpendicular orientations. The vertical dotted line defines the crossover frequency $\omega_{\text{Pd-PI}}^*$ at which $G^*(\text{PI}) = G^*(\text{Pd})$. Following work by Patel et al.,¹⁰ the LAOS conditions are superimposed on these master curves by shifting the applied LAOS frequency (1 rad/s) by shift factors, a_T , corresponding to T_{LAOS} . Each LAOS condition is designated by a triangle (∇) and further denoted by T_{LAOS} and the resultant morphology.

For the blended specimens, f_R and f_{SAXS} agree exactly; however, for the neat specimens, f_R and f_{SAXS} disagree substantially. It was noted previously that these samples contain lamellae in orientations between the parallel and perpendicular orientations. Inspection of the SAXS data in parts a and b of Figure 4, indicates that the mixed morphologies for the neat system contain considerably more lamellae at orientations between the parallel and perpendicular orientations than does the blended system. It follows then that the results from the specimen with more lamellae in intermediate orientations, namely, the neat specimen, would be inconsistent with an analysis which is based on the parallel and perpendicular orientations only. Another caveat regarding this analysis involves our new SAXS and TEM findings, which indicate that specimens nominally in the perpendicular orientation have a region ($\sim 2\text{--}10\ \mu\text{m}$) near the shearing surfaces which contains lamellae in the parallel orientation.²⁵ This parallel orientation at the surface would alter the analyses of both f_R and f_{SAXS} . Last, the disparity in the fractional contributions of the parallel orientation could arise from the existence of a nonlinear relationship between the amount of a morphological orientation present and the influence of that orientation on the rheological response, perhaps due to a nonuniform strain field.

Relation of LAOS Conditions to the Induced Macroscopic Morphologies. In a study on a similar low- M_w SI diblock (SI(12-9)), Patel et al.¹⁰ show evidence that the lamellar orientation macroscopically induced at a given temperature and frequency coincides with the orientation that has the lower linear viscoelastic complex modulus G^* at that same temperature and frequency. In Figure 8, Patel's analysis has been applied to our data for SI(11-10) by displaying master curves of G^* for the perpendicular and parallel orienta-

tions at a reference temperature of 100 °C. A crossover frequency, $\omega_{\text{Pd-PI}}^*$, is identified which corresponds to the frequency where the curves for the parallel and perpendicular orientations intersect. (As will be discussed later in this paper, this crossover frequency is not the critical frequency, ω_c , used by others to correlate the applied LAOS and the resultant block copolymer morphology.) The LAOS conditions are added to these master curves by shifting the applied frequency ($\omega = 1$ rad/s) by a_T , where this shift factor is that of the unaligned state evaluated at the temperature used during LAOS, T_{LAOS} . As Patel et al. argued, the shift factors for the unaligned state were used because the samples are in the unaligned state when LAOS is initially applied.¹⁰ Each LAOS reduced frequency is designated by a triangle and denoted with T_{LAOS} and the observed morphology. Except for the observation of the mixed morphologies (M) near the crossover frequency, $\omega_{\text{Pd-PI}}^*$, our results concur with the findings of Patel. A probable explanation for why Patel et al. did not observe the mixed morphologies is that, because they used larger temperature increments (10 °C), their LAOS conditions straddled those which may have induced the mixed morphology. For our system, the conditions which induce the mixed morphology span a temperature range of $\sim 10\text{--}15\ ^\circ\text{C}$ at a constant frequency, as will be discussed further in the following paragraphs. In addition, they employed photographic film for the collection of their SAXS patterns which may not have provided sufficient sensitivity to detect a mixed morphology which was predominately parallel or perpendicular. In a subsequent paper they report in passing the observation of a mixed parallel-perpendicular morphology.¹¹

The failure of Patel's analysis using only the G^* data to account for the mixed morphologies led us to generate a similar construction using both the G' and G'' data. Figure 9 displays master curves of G' and G'' for the parallel and perpendicular orientations of SI(11-10) at a reduced temperature of 125 °C. Time-temperature superposition was applied to the two orientations separately, using the shift factors appropriate for each aligned state. From these master curves two crossover frequencies, $\omega_{\text{Pd-PI}}'$ and $\omega_{\text{Pd-PI}}''$, are identified which correspond to the frequencies where the data for the parallel and perpendicular orientations intersect. At frequencies higher than $\omega_{\text{Pd-PI}}'$ the parallel orientation has the lower moduli, while at frequencies below $\omega_{\text{Pd-PI}}''$ the perpendicular orientation has the lower moduli. Note that $\omega_{\text{Pd-PI}}' > \omega_{\text{Pd-PI}}''$, thus, these two crossover frequencies divide frequency into three regimes: $\omega < \omega_{\text{Pd-PI}}''$, $\omega_{\text{Pd-PI}}'' < \omega < \omega_{\text{Pd-PI}}'$, and $\omega > \omega_{\text{Pd-PI}}'$. The crossover frequencies determined in Figure 9 correspond to 125 °C. Using the temperature dependence of the shift factors, additional master curves were generated having reference temperatures between 100 and 120 °C. From this series of isothermal master curves the temperature dependence of the crossover frequencies was determined as plotted in Figure 10a.

In addition to the two crossover frequencies, $\omega_{\text{Pd-PI}}'$ and $\omega_{\text{Pd-PI}}''$, the LAOS conditions are plotted (T_{LAOS} , $\omega = 1$ rad/s) in Figure 10a and labeled with the resultant morphologies. The parallel orientation is observed when LAOS is applied at a temperature such that the

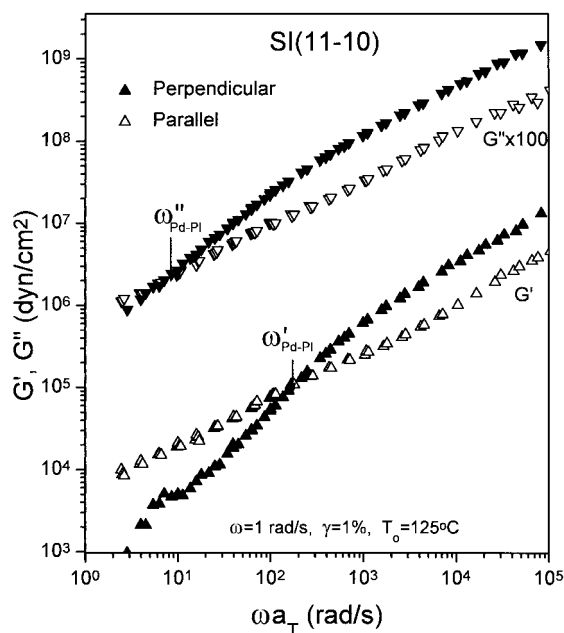


Figure 9. Master curves of G' and G'' as a function of frequency at a reference temperature of 125 °C. Data are for SI(11-10) in the parallel and perpendicular orientations. The G'' data have been shifted vertically for clarity. Two crossover frequencies, ω_{Pd-PI}' and ω_{Pd-PI}'' , are determined at which $G'(\text{PI}) = G'(\text{Pd})$ and $G''(\text{PI}) = G''(\text{Pd})$, respectively.

frequency of the LAOS is greater than both ω_{Pd-PI}' and ω_{Pd-PI}'' . This corresponds to the situation where the parallel orientation has both a lower storage (G') and loss moduli (G'') in the linear viscoelastic regime than the perpendicular orientation. Similarly, the perpendicular orientation is observed when the frequency of LAOS is less than both ω_{Pd-PI}' and ω_{Pd-PI}'' , corresponding to the linear viscoelastic region where the perpendicular orientation has the lower G' and G'' . When LAOS is applied in the range between ω_{Pd-PI}' and ω_{Pd-PI}'' , i.e., where the perpendicular orientation has a lower G' but the parallel orientation has a lower G'' in the linear viscoelastic region, a mixed morphology is produced which contains both of these orientations. Further, the relative amounts of each orientation observed in the mixed morphologies is coincident with its proximity to the $\omega_{Pd-PI}'(T)$ and $\omega_{Pd-PI}''(T)$ boundaries shown in Figure 10a. For example, at 110 °C the LAOS condition is closer to the $\omega_{Pd-PI}'(T)$ boundary which separates the mixed and the parallel regions and thus exhibits a greater fraction of the parallel orientation (Table 1).

Figure 10b contains the same analysis as was described above, but in this case the specimen is the SI(11-10)/hS(13) 10% blend. All the observations discussed for the neat system apply to the blend.

Comparison with Theoretical Results. The phenomenological basis for shear-induced macroscopic alignment in copolymer melts has received some theoretical attention. An earlier theory by Cates and Milner,²⁶ which predicts the occurrence of the perpendicular orientation, was recently modified by Fredrickson²⁷ to incorporate the effect of the different viscosities of the two microdomains. One of the results of Fredrickson's field theory is to show that a transition temperature (τ_p) exists, above which strong shearing induces the perpendicular orientation and below which strong shearing induces the parallel orientation. The minimization of

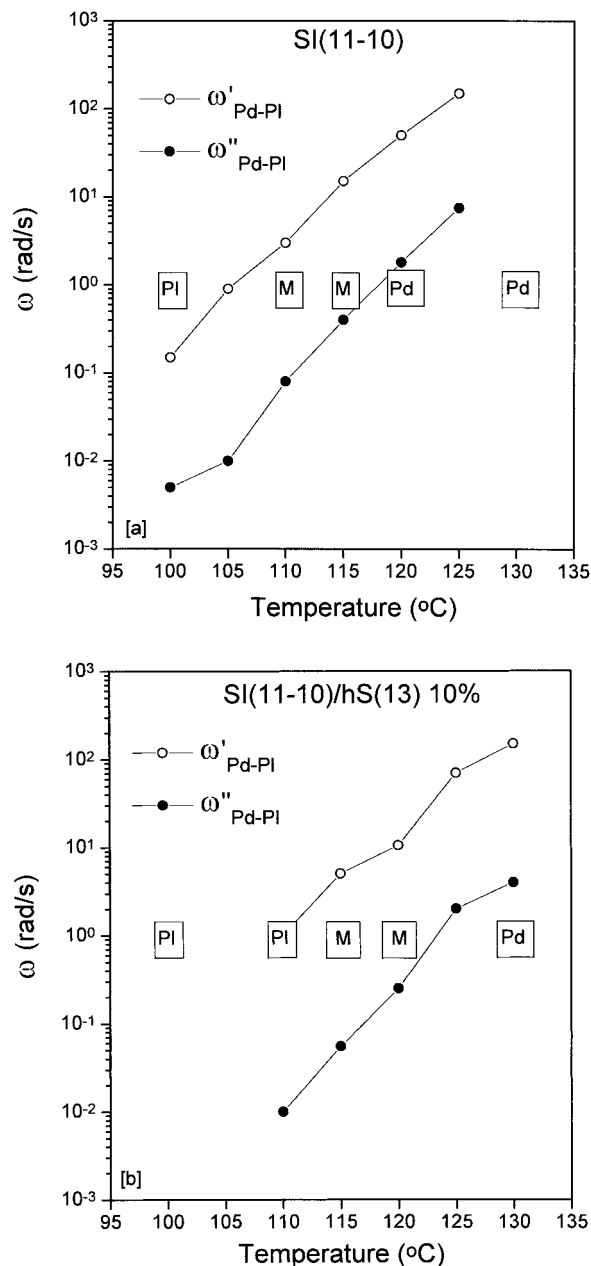


Figure 10. Temperature dependence of the crossover frequencies, ω_{Pd-PI}' and ω_{Pd-PI}'' , for (a) SI(11-10) and (b) SI(11-10)/hS(13) 10%. Included in the plots are designations for the LAOS conditions (T_{LAOS} , 1 rad/s) used to produce the indicated morphologies.

a constructed potential Φ dictates the steady-state orientation obtained in the sheared copolymer melt. The salient features are summarized here and are illustrated schematically in Figure 11. Upon cooling a copolymer melt from above the order-disorder transition (ODT) temperature while it is being subjected to strong shear, the potential for the perpendicular orientation, Φ_{Pd} , becomes less than zero at T_{ODT} and a spinodal instability to perpendicular lamellae occurs. With further cooling the potential for the parallel orientation, Φ_{PI} , becomes less than zero at the stability limit for the parallel orientation, τ_{sy} , but the perpendicular orientation persists because $\Phi_{Pd} < \Phi_{PI}$. Cooling still further decreases Φ_{PI} below Φ_{Pd} at τ_p , and a transition should occur from perpendicular to parallel lamellae. The transition temperature τ_p could theoretically be determined by fitting the angular dependence

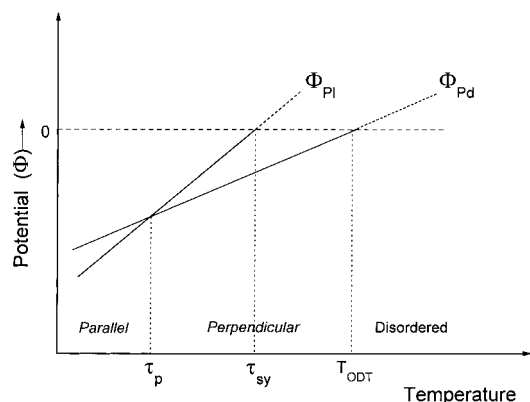


Figure 11. Schematic depicting the temperature dependence of the potential for lamellae in the parallel (Φ_{Pl}) and perpendicular (Φ_{Pd}) orientations during strong shearing.²⁷

of the quadratic coefficient (cf. eq 2.28 of ref 17) to Leibler's numerical calculations.²⁸ Such a fitting exercise is beyond the scope of this work, and therefore a quantitative comparison with the theory will not be made.

The origin of the mixed morphologies may relate to the temperature regime in the Fredrickson theory where $\tau_p < \tau < \tau_{sy}$, which is below the stability limit for the parallel orientation yet where the perpendicular orientation still represents the systems minimum potential ($\Phi_{Pd} < \Phi_{Pl} < 0$). The above discussion of the Fredrickson theory was for a specimen which was cooled from the homogeneous state, above the ODT, while shearing was applied. In contrast, our specimens are cooled below the ODT to form an isotropic microphase-separated state *before* shear is applied. These isotropic samples necessarily contain some fraction of lamellae in and near the parallel orientation. According to Fredrickson, the effective shear rate is larger for lamellae in the parallel orientation than for those in the perpendicular orientation because in the parallel orientation the softer lamellae, having a lower viscosity, will respond by flowing at a higher rate. As well, composition fluctuations about the parallel orientation experience an increased effective shear rate and are more strongly suppressed than fluctuations about the perpendicular orientation. These mechanisms could stabilize the parallel orientation relative to the perpendicular orientation and thus prevent the elimination of the parallel orientation at $\tau_p < \tau < \tau_{sy}$. The absence of "reverse flipping" (parallel to perpendicular) supports this explanation. An additional possibility, considered separately or in conjunction with the previous one, is that since both orientations are below their stability limit in the region $\tau_p < \tau < \tau_{sy}$, the driving force for lamellae in the parallel orientation to become perpendicular could be quite small. Therefore, even though in this region the perpendicular orientation corresponds to the minimum of the systems potential and should be theoretically achieved, the practical duration of experiments may not provide sufficient time for the system to be considered ergodic. This discussion supports other evidence that the nuances of the initial morphology can substantially influence the resultant morphology, as we will discuss below.

Comparison with Other Experimental Results.

The collective effort of the research community to understand block copolymer alignment is hampered, in part, by the difficulties of characterizing the resulting

morphology in a manner which allows straightforward comparisons to be made between research groups. In this paper we use small-angle X-ray scattering (SAXS), but we have elected not to calculate order parameters using the methods put forth by Ehlich et al.²⁹ and used by Zhang and Wiesner.¹⁵ The order parameter applied by these authors assumes fiber symmetry which is inappropriate for lamellar microdomains. The characterization of the morphology by SAXS is also dependent somewhat on the specific experimental apparatus setup. For example, there should be *zero* Bragg scattering from *perfectly* aligned material when the incident X-ray beam is *exactly* perpendicular to the lamellae normals. Experimentally, however, specimens are mosaic and X-ray beams are not perfectly collimated, so that much of the beam is able to meet the Bragg condition. Beam divergence depends on the details of the collimation system and so varies between labs. Thus, comparing final morphologies and appropriate order parameters between research groups reflects, in part, the extent of order in the sample but is convoluted with the precise sample orientation relative to the beam and the beam divergence.

The collective effort is also hampered by the sensitivity of the final morphology to the initial morphology and the variety of initial morphologies employed. Consider, for example, our recent work investigating kink bands in high molecular weight lamellar diblock copolymers.³⁰ Depending on the initial state used (with or without preliminary shearing at 20% shear strain amplitude), identical large-amplitude shearing conditions (40% strain at 1 rad/s for 6 h) could either create a uniaxial parallel orientation or a parallel-transverse biaxial texture, corresponding to conjugate kink bands.^{12,30} Therefore, even though the materials and alignment procedures might be similar between research groups, frequently the details of preparing the "initial morphologies" differ. In this paper our protocol for preparing the initial state is similar to (but not exactly) that used by Chen et al.¹³ Like Chen et al., we raise the temperature above the order-disorder temperature, T_{ODT} , to erase all prior morphologies. Then we quench to a fixed temperature, while Chen et al. quench to the temperature used during the subsequent LAOS. We have elected to quench to the same temperature for each experiment, because quench depth ($T - T_{ODT}$) will certainly influence the resultant morphology.³¹ Once our quenched morphology is established, we move to our LAOS temperature and proceed. In contrast, Zhang and Wiesner¹⁵ elected not to exceed the T_{ODT} in preparing their specimens, and consequently we need to limit our comparisons to their data.

Some research groups have taken to reporting their alignment conditions as a reduced temperature, T/T_{ODT} , where T is the temperature of LAOS. This practice implies that at a given reduced temperature a particular type of macroscopic orientation will be induced in all systems. A review of shear-induced alignments reported in the literature, along with our present results, demonstrates that the LAOS conditions to induce the parallel and perpendicular orientations are, in fact, system specific. The transition temperature τ_p described in Fredrickson's theory which separates the parallel and perpendicular alignment regimes is dependent not only on its relative proximity to the ODT but also on the viscosities of the microdomains in the system, which, in turn, depend on temperature, molec-

ular weight, and monomeric units. Therefore, the viscosities at the LAOS temperature as well as the proximity to T_{ODT} should be taken into account when predicting the type of orientation to be induced.

We shall now endeavor to associate our results with the recent publications by Chen et al.^{13,14} Note that the differences between our materials and in the preparation of our initial morphologies are subtle. While we have elected to define $\omega_{\text{Pd-P1}}'$ and $\omega_{\text{Pd-P1}}''$ as the frequencies of interest, Chen et al. have used ω_c' , which is defined as the frequency at which the linear viscoelastic response diverges between the high-temperature disordered state and the lower temperature ordered state. See, for example, Figure 3 of ref 13. To define this critical frequency, one must assume a well-behaved shift factor. This critical frequency can also be difficult to determine due to the limited range of accessible experimental frequencies, which in some cases results in the failure of the data to intersect. Furthermore, the critical frequency depends on the state of alignment of the specimen; compare Figures 1, 3, and 4 of ref 10. In contrast, if one can produce the parallel and perpendicular orientations, the crossover frequencies $\omega_{\text{Pd-P1}}'$ and $\omega_{\text{Pd-P1}}''$ are straightforward to determine.

Patel et al. previously commented that for these low molecular weight SI diblock copolymers $a_T \omega_{\text{Pd-P1}}'$ is approximately equal to $a_T \omega_c'$.¹⁰ Thus, we can compare our results to those in Figure 2 of ref 13 by assuming that $a_T \omega_{\text{Pd-P1}}'$ equals $a_T \omega_c'$. Chen et al. describe three temperature-independent regimes which describe the sequence of morphologies induced by LAOS: regime I ($\omega/\omega_c \lesssim 0.9$) isotropic to mixed parallel-perpendicular to perpendicular; regime II ($0.9 \lesssim \omega/\omega_c \lesssim 8$), isotropic to mixed parallel-perpendicular to parallel; regime III ($\omega/\omega_c \gtrsim 8$), isotropic to mixed parallel-transverse to parallel. For this study on SI(11-10), the lowest relative frequencies ($\omega/\omega_{\text{Pd-P1}}'$) of 0.0025 (130 °C) and 0.02 (120 °C) correspond to the perpendicular orientation, as expected in regime I. The highest relative frequency studied, 6.7 (100 °C), produces the parallel orientation which is consistent with either regime II or III. Finally, the intermediate relative frequencies of 0.067 (115 °C) and 0.5 (110 °C) produced mixed morphologies which are consistent with the intermediate, rather than the final, stage of regime I. This could imply that our mixed morphology specimens did not obtain a steady state during LAOS. However, as stated previously, longer durations of shear (increased by a factor of 3) did not alter the rheological response or final morphology obtained at these intermediate relative frequencies. The observed discrepancy could also be attributed to differences in the initial morphology associated with ordering the samples at different temperatures. In conclusion our results are not inconsistent with the work by Chen et al.¹³

This comparison between the results from two research groups reveals two interesting points. First, the issue of the duration of LAOS needs to be addressed. At both low and high relative frequencies, our LAOS conditions produced uniaxial morphologies, while at intermediate relative frequencies our resultant morphology was mixed parallel-perpendicular. Chen et al. have already demonstrated that applying a greater strain amplitude will hasten the production of the ultimate morphology.¹³ However, at a fixed strain amplitude the duration of LAOS necessary to produce a uniaxial morphology apparently depends nonmono-

tonically on the relative frequency. Second, it appears to be inconsequential whether one chooses to calculate the relative frequency with respect to ω_c or $\omega_{\text{Pd-P1}}$. Thus, the origins of the morphologies cannot be unequivocally assigned to either the transition from probing molecules to probing microdomains as defined by ω_c or the transition from producing a smaller modulus for the parallel orientation to producing a smaller modulus for the perpendicular orientation as defined by $\omega_{\text{Pd-P1}}$. In other words, the following question still exists: Is the alignment controlled by the length scales on which the shearing acts and/or is it controlled by the viscoelastic properties of the system?

V. Conclusion

For both a low molecular weight SI diblock copolymer and its blend with hS, applying LAOS at high temperatures, relative to the range between T_g and T_{ODT} , induces the perpendicular orientation and applying LAOS at sufficiently low temperatures induces the parallel orientation. LAOS conditions between those that induce the parallel and perpendicular orientations induce a mixed morphology which contains predominately the parallel and perpendicular orientations, along with a smaller fraction of orientations intermediate between the two. The rheological response of these mixed morphologies can be fit by a linear combination of the rheological responses of the parallel and perpendicular orientations.

In this study we have attempted to contribute to the effort to understand block copolymer alignment by focusing on the correlations between the linear viscoelastic responses and the applied LAOS conditions. We have refined the earlier work of Patel et al.¹⁰ by employing both the storage and loss moduli (instead of just the complex modulus) to identify two temperature-dependent crossover frequencies, $\omega_{\text{Pd-P1}}'$ and $\omega_{\text{Pd-P1}}''$, corresponding to where the linear viscoelastic moduli for the parallel and perpendicular orientations are equal. These crossover frequencies define three, rather than two, regimes in LAOS conditions corresponding to the production of the perpendicular, the parallel, and the mixed parallel-perpendicular morphologies. We have shown that the orientation induced by LAOS corresponds to that which has the lower linear viscoelastic storage and loss moduli at the temperature and frequency of the strong shearing. Applying LAOS at conditions where the linear viscoelastic response of the parallel orientation has a lower G' and the perpendicular orientation has a lower G'' induces a mixed morphology of the parallel and perpendicular orientations.

Finally, comparison of our results with theoretical predictions supports the concept that viscoelastic contrast is significant to determine the type of orientation induced. Comparison of our results with other experimental work indicates that ω_c' and $\omega_{\text{Pd-P1}}'$ can be interchanged, thereby leaving open to interpretation the driving forces of block copolymer alignment.

Acknowledgment. This work was supported, in part, by NSF-IMR (93-05286), NSF-MRSEC-DMR (96-32598), and the University Research Foundation. B.S.P. is grateful for support from an Ashdon Fellowship, and K.I.W. is grateful for support from NSF-YIA (94-57997). K.I.W. is grateful for discussions with Prof. N. P. Balsara and Prof. J. A. Kornfield.

References and Notes

- (1) Folkes, M. J.; Keller, A.; Scalisi, F. P. *Colloid & Polym. Sci.* **1973**, *251*, 1.
- (2) Hadziioannou, G.; Mathis, A.; Skoulis, A. *Colloid Polym. Sci.* **1979**, *257*, 15.
- (3) Morrison, F.; Bourvellec, G. I.; Winter, H. H. *J. Appl. Polym. Sci.* **1987**, *33*, 1585.
- (4) Scott, D. B.; Waddon, A. J.; Lin, Y.-G.; Karasz, F. E.; Winter, H. H. *Macromolecules* **1992**, *25*, 4175.
- (5) Koppi, K. A.; Tirrell, M.; Bates, F. S.; Almdal, K.; Colby, R. H. *J. Phys. II Fr.* **1992**, *2*, 1941.
- (6) Winey, K. I.; Patel, S. S.; Larson, R. G.; Watanabe, H. *Macromolecules* **1993**, *26*, 4373.
- (7) Winey, K. I.; Patel, S. S.; Larson, R. G.; Watanabe, H. *Macromolecules* **1993**, *26*, 2542.
- (8) Kannan, R. M.; Kornfield, J. A. *Macromolecules* **1994**, *27*, 1177.
- (9) Okamoto, S.; Saijo, K.; Hashimoto, T. *Macromolecules* **1994**, *27*, 5547.
- (10) Patel, S. S.; Larson, R. G.; Winey, K. I.; Watanabe, H. *Macromolecules* **1995**, *28*, 4313.
- (11) Riise, B. L.; Fredrickson, G. H.; Larson, R. G.; Pearson, D. S. *Macromolecules* **1995**, *28*, 7653.
- (12) Pinheiro, B. S.; Winey, K. I.; Hajduk, D. A.; Gruner, S. M. *Macromolecules* **1996**, *29*, 1482.
- (13) Chen, Z.-R.; Issaian, A. M.; Kornfield, J. A.; Smith, S. D.; Grothaus, J. T.; Satkowski, M. M. *Macromolecules* **1997**, *30*, 7096.
- (14) Chen, Z.-R.; Kornfield, J. A.; Smith, S. D.; Grothaus, J. T.; Satkowski, M. M. *Science* **1997**, *277*, 1248.
- (15) Zhang, Y.; Wiesner, U. *J. Chem. Phys.* **1997**, *106*, 2961.
- (16) Kornfield, J. A.; Kannan, R. M.; Smith, S. *Prepr.-Am. Chem. Soc.* **1994**, *34*, 676.
- (17) Gupta, V. K.; Krishnamoorti, R.; Chen, Z.-R.; Kornfield, J. A.; Smith, S. D.; Satkowski, M. M.; Grothaus, J. T. *Macromolecules* **1996**, *29*, 875.
- (18) Gupta, V. K.; Krishnamoorti, R.; Kornfield, J. A.; Smith, S. D. *Macromolecules* **1996**, *29*, 1359.
- (19) Wiesner, U. *Macromol. Chem. Phys.* **1997**, *198*, 3319.
- (20) Balsara, N. P.; Perahia, D.; Safinya, C. R.; Tirrell, M.; Lodge, T. P. *Macromolecules* **1992**, *25*, 3896.
- (21) Pinheiro, B. S.; Winey, K. I. *J. Rheology* **1998**, submitted.
- (22) Pinheiro, B. S. In *Rheology and Morphology of Shear Induced Orientation in Diblock Copolymer/Homopolymer Blends*; Pinheiro, B. S., Ed.; University of Pennsylvania: Philadelphia, PA, 1996; p 194.
- (23) Owens, J. N.; Gancarz, I. S.; Koberstein, J. T.; Russell, T. P. *Macromolecules* **1989**, *22*, 3388.
- (24) Pinheiro, B. S.; Winey, K. I. *Polym. Prepr.* **1995**, *36*, 174.
- (25) Pinheiro, B. S.; Laurer, J. H.; Grothaus, J.; Satkowski, M. M.; Winey, K. I. *Macromolecules* **1998**, in preparation.
- (26) Cates, M. E.; Milner, S. T. *Phys. Rev. Lett.* **1989**, *62*, 1856.
- (27) Fredrickson, G. H. *J. Rheol.* **1994**, *38*, 1045.
- (28) Leibler, L. *Macromolecules* **1980**, *13*, 1602.
- (29) Ehlich, D.; Takenaka, M.; Okamoto, S.; Hashimoto, T. *Macromolecules* **1993**, *26*, 189.
- (30) Polis, D. L.; Winey, K. I. *Macromolecules* **1998**, *31*, 3617.
- (31) Newstein, M. C.; Garetz, B. A.; Balsara, N. P.; Chang, M. Y.; Dai, H. J. *Macromolecules* **1998**, *31*, 64.

MA980186A